Fig. 1

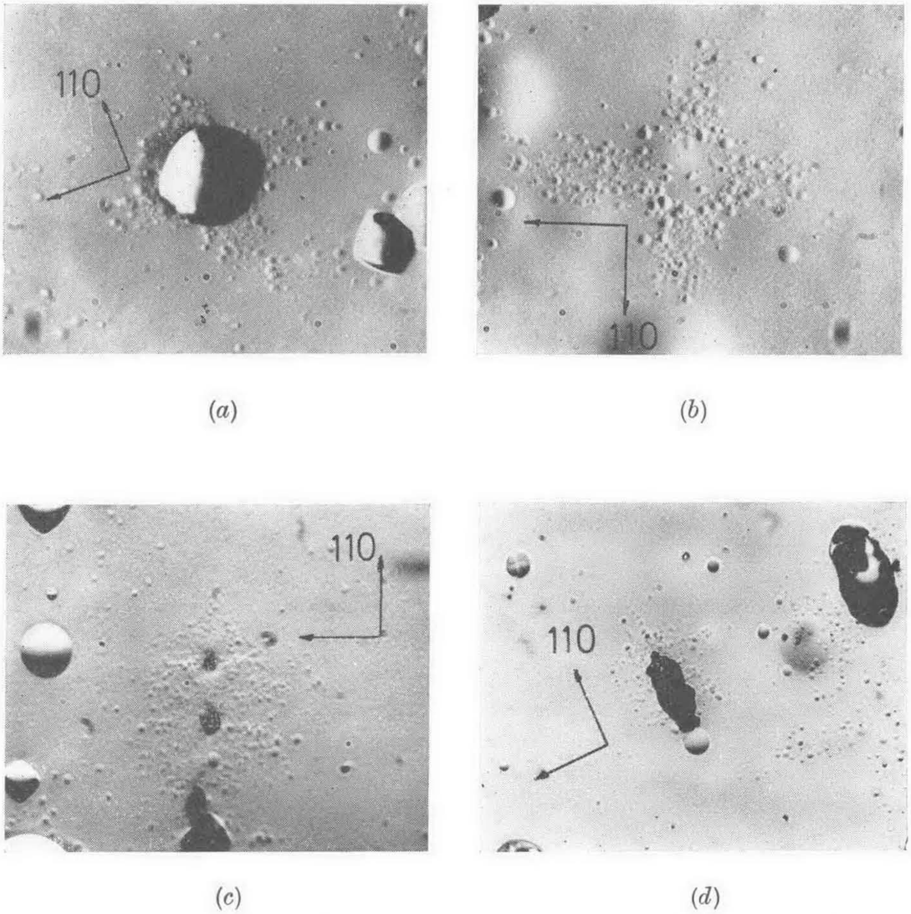

Dislocation etch-pits at particles in a chromium single crystal after pressurization at 9 kbars. The etching plane is (001). Magn. $\sim \times 700$.

of the $\langle 111 \rangle$ slip directions on the surface. The occasional observation of etch-pit clouds when the particle was either above or below the etched surface plane (e.g. fig. 1*b*) was also consistent with the emanation of dislocations in directions inclined to the surface, such as $\langle 111 \rangle$.

Electron micrographs usually show considerable dislocation tangling around particles and the classical arrangement of fig. 2 is rather unusual. The helical dislocations (fig. 2) are typical of prismatic punching (Jones and Mitchell 1958) and the loop spacing, of the order of the loop diameter, is consistent with the behaviour of prismatic dislocations (Bullough and Newman 1960) ; the loops are emitted in $\langle 111 \rangle$ directions.

Both polycrystals and single crystals contained particles, up to 20 microns in diameter, usually in stringers parallel to the wire axis. Electropolishing and etching increased the apparent particle size. However, mechanical polishing and repeated sectioning showed that only particles of diameters greater than about 0·2 microns generated dislocations at 9 kbars.

Fig. 2

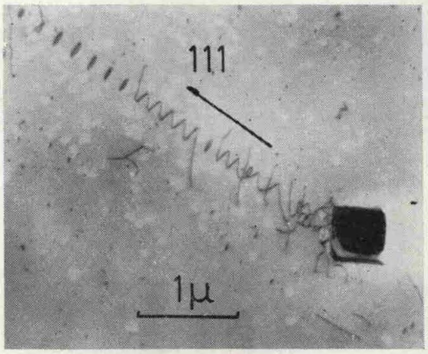

A classical prismatic dislocation source, observed by transmission electron microscopy, in polycrystalline chromium after pressurization at 15 kbars.

X-ray diffraction photographs of the non-metallic residue from the dissolution of the chromium in hot hydrochloric acid showed the major constituent to be the stable (hexagonal) oxide Cr_2O_3.

3.2. *The Nature of the Prismatic Loops*

Prismatic punching can produce either vacancy or interstitial dislocation loops according to whether the stress differential at the particles is tensile or compressive. Contrast analysis, using a method devised by Edmondson and Williamson (1964), shows that the present loops are of vacancy type.

This method involves noting the variation in the minor axis of the elliptical image of the loop as the specimen is tilted continuously in one direction, through a large angle, about an axis parallel to the major axis of the loop. The minor axis changes both geometrically and because of a variation in diffraction contrast with the sign of the product $(\mathbf{g}\,.\,\mathbf{b})\mathbf{s}$. In fig. 3 the Burgers vector ($\mathbf{b}$) is known from ‘ invisibility ’ conditions to lie in the [111] direction parallel to the row of loops ; the deviation from exact Bragg conditions in reciprocal space ($\mathbf{s}$) is set positive for all micrographs and the direction of $\mathbf{g}$, the reciprocal lattice vector for the particular operating reflections, and the sense and degree of inclination of the foil are shown. It follows from the gross change in their minor axes with tilt (from $+14°$ to $-10°$) that the two loops marked + lie with opposite inclination